

## Quantum Degenerate Fermi–Bose Mixtures of $^{40}\text{K}$ and $^{87}\text{Rb}$ Atoms in a Quadrupole-Ioffe Configuration Trap

This content has been downloaded from IOPscience. Please scroll down to see the full text.

2008 Chinese Phys. Lett. 25 843

(<http://iopscience.iop.org/0256-307X/25/3/011>)

View [the table of contents for this issue](#), or go to the [journal homepage](#) for more

Download details:

IP Address: 169.229.32.36

This content was downloaded on 14/08/2015 at 20:00

Please note that [terms and conditions apply](#).

## Quantum Degenerate Fermi–Bose Mixtures of $^{40}\text{K}$ and $^{87}\text{Rb}$ Atoms in a Quadrupole-Ioffe Configuration Trap \*

XIONG De-Zhi(熊德智), CHEN Hai-Xia(陈海霞), WANG Peng-Jun(王鹏军), YU Xu-Dong(于旭东),  
GAO Feng(高峰), ZHANG Jing(张靖)\*\*

State Key Laboratory of Quantum Optics and Quantum Optics Devices, Institute of Opto-Electronics,  
Shanxi University, Taiyuan 030006

(Received 26 September 2007)

We report on the attainment of quantum degeneracy of  $^{40}\text{K}$  by means of efficient thermal collisions with the evaporatively cooled  $^{87}\text{Rb}$  atoms. In a quadrupole-Ioffe configuration trap, potassium atoms are cooled to 0.5 times the Fermi temperature. We obtain up to  $7.59 \times 10^5$  degenerate fermions  $^{40}\text{K}$ .

PACS: 03.75.Hh, 05.30.Fk, 05.30.Jp, 32.80.Pj

In recent years, experimental and theoretical studies on quantum degenerate Fermi gases (DFG) and quantum degenerate Bose–Fermi mixtures (BFMs) have attracted much attention.<sup>[1,2]</sup> The observation of Bose–Einstein condensation and Fermi degenerate gases promises further understanding of high- $T_c$  superconductivity, strong interaction, and investigation of quantum degenerate many-body systems. The experimental development in this field has been made by utilizing a number of important tools, such as optical dipole traps,<sup>[3]</sup> optical lattices<sup>[4]</sup> and magnetic control of inter atomic potentials<sup>[5]</sup> available to a larger community.

degenerate Fermi gas  $^{40}\text{K}$  by evaporatively cooling bosonic  $^{87}\text{Rb}$  atoms in a quadrupole-Ioffe configuration (QUIC) trap.<sup>[6]</sup> We have achieved the numbers of fermions, up to  $7.59 \times 10^5$  atoms, and  $^{40}\text{K}$  quantum Fermi degeneracy characterized by a temperature of one-half the Fermi temperature. This provides us with the starting point for studies of the degenerate  $^{40}\text{K}$  Fermi gas. Furthermore, favourable collision properties make the  $^{40}\text{K}$ - $^{87}\text{Rb}$  system very promising for studies of quantum degenerate Bose–Fermi mixtures.

The standard techniques of laser cooling and trapping are required for the experiment in achieving quantum degenerate gases. In our case, a double magneto-optical-trap (MOT) system, schematically shown in Fig.1, is utilized to cool and trap both atomic species, and then the cold atom samples are transferred into the QUIC trap, where we cool potassium to the degenerate regime by performing selective evaporative cooling on the rubidium component. The potassium dispensers and commercial rubidium source are constructed according to Ref. [7]. The complexity of our apparatus is increased with respect to the single species setup because we have to cool and trap simultaneously two different atomic species. In particular, since the two transitions, at 780 nm and 767.7 nm for  $^{87}\text{Rb}$  and  $^{40}\text{K}$  respectively, are necessary, we use a semiconductor laser system for potassium and rubidium, which has been described in detail previously.<sup>[8]</sup>

The double MOTs are produced in collection cell and science cell respectively. The collection cell, designed to capture atoms from a background vapour, is a compact octagonal chamber with eight CF35 viewpoints in the horizontal plane, and two

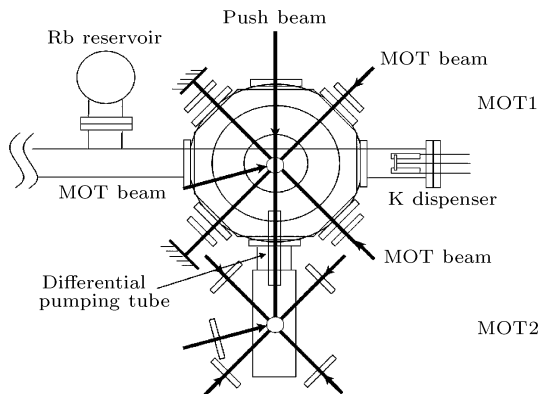


**Fig. 1.** Experimental apparatus: atoms of both species are cooled and trapped in MOT1 and then transferred in MOT2, where they are magnetically trapped. In the magnetic trap, the potassium sample is cooled to quantum degeneracy by means of efficient elastic collisions with the evaporatively cooled  $^{87}\text{Rb}$ .

In this Letter, we report the production of a

\*Supported in part by the National Basic Research Programme of China under Grant No 2006CB921101, the National Natural Science Foundation of China for Distinguished Young Scholars under Grant No 10725416, the National Natural Science Foundation of China under Grant No 60678029, the Programme for New Century Excellent Talents in University under Grant No NCET-04-0256, the Specialized Research Fund for the Doctoral Programme of Higher Education of China under Grant No 20050108007, the Cultivation Fund of the Key Scientific and Technical Innovation Project, Ministry of Education of China under Grant No 705010, the Programme for Changjiang Scholars and Innovative Research Team in University, the Natural Science Foundation of Shanxi Province under Grant No 2006011003, and the Research Fund for the Returned Abroad Scholars of Shanxi Province.

\*\*To whom correspondence should be addressed. Email: jzhang74@sxu.edu.cn or jzhang74@yahoo.com

CF100 viewpoints in the vertical direction. The science cell is a quartz glass cell with inner size  $30\text{ mm} \times 30\text{ mm} \times 90\text{ mm}$ , which allows for trapping beams with a diameter of 2.5 cm to capture a large number of atoms.

In the case of the MOT1, we use three retroreflected beams along the  $X-Y-Z$  spatial directions.<sup>[9]</sup> Instead, the second MOT configuration (MOT2) uses six beams in all the three directions, whose intensity can be independently regulated by polarizing cubes and half-wave plates. We set the six beams to maximize the loading of the MOT and the mode-matching with the magnetic trap. The light for double MOTs is provided by two tapered amplifiers (TAs). The cooling and repumping light for the rubidium and potassium atoms is provided by four slave injected-locked lasers.<sup>[8]</sup> Then the rubidium cooling light is amplified by the first tapered amplifier (TA1), and the potassium cooling and repumping light is also amplified simultaneously by the second tapered amplifier (TA2). The ratio of laser power for potassium cooling and repumping is 3:1. After amplification, the light for potassium is combined with the light for rubidium with the polarizing beam splitter cubes. Then this light is divided into two parts, one is for MOT1 and the other for MOT2. The laser power for MOT1 is 150 mW for  $^{87}\text{Rb}$  and 60 mW for  $^{40}\text{K}$ , and the laser power of 110 mW for  $^{87}\text{Rb}$  and 80 mW for  $^{40}\text{K}$  is used by MOT2.

The first MOT is loaded from samples of bosonic  $^{87}\text{Rb}$  and of fermionic  $^{40}\text{K}$  in the vacuum chamber at the pressure of  $5.0 \times 10^{-7}\text{ Pa}$ . The numbers of atoms loaded individually into the MOT1 are  $10^9-10^{10}$  for  $^{87}\text{Rb}$  and  $10^7-10^8$  for  $^{40}\text{K}$ . Then we transfer the atoms of the two species from MOT1 to MOT2 by pulse pushing beam, whose mark-space ratio is 1:10 in every 500 ms. In MOT2 where the vacuum is kept at  $3.0 \times 10^{-9}\text{ Pa}$ , we can obtain about  $10^9$   $^{87}\text{Rb}$  atoms and about  $10^7$   $^{40}\text{K}$  atoms, respectively, which are transferred in about 30 s from MOT1.

In addition, we observe a strong performance reduction of a  $^{40}\text{K}$  MOT in the presence of the rubidium cloud, first reported in Ref. [10]. This is attributed to strong light-assisted heteronuclear collisions in the MOT. To optimize the  $^{40}\text{K}$  atoms numbers, we use a little strategy as follows. In the loading of the two-species MOT, we adopt two-step loading. First we load  $^{40}\text{K}$  atoms alone about 30 s, and the Rubidium cooling and repumping light are blocked. Then with keeping the  $^{40}\text{K}$  loading, we took a fast  $^{87}\text{Rb}$  loading within 10 s. The two-step loading has provided maximum particle numbers in our experiment.

After the loading of MOT2, the temperature of the atoms is brought close to the recoil limit in an optical molasses phase. In a second preparation step the atoms are optically pumped in their polarized spin state,  $|F = 9/2, m_F = 9/2\rangle$  for  $^{40}\text{K}$  and  $|F = 2, m_F =$

$2\rangle$  for  $^{87}\text{Rb}$ . Then atoms are captured in a magnetic quadrupole field induced by two MOT2 coils. Then the current of these coils is ramped up from 15 A to 25 A in 600 ms, which compresses the cold ensemble. Subsequently, the quadrupole potential is converted into a harmonic trapping potential, produced by a magnetic trap in QUIC configuration, in which we start to perform the evaporation.

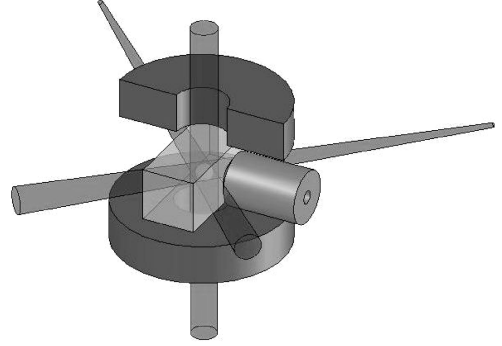


**Fig. 2.** Dual-species MOT2 formed at the intersection of six laser beams. After molasses and optical pumping, the Ioffe coil (purple) converts the spherical quadrupole trap into an Ioffe configuration trap with its trap centre close to the Ioffe coil.

Figure 2 shows the QUIC trap utilized in our experiment. It consists of a pair of coils in anti-Helmholtz configuration with 288 turns with a separation of 40 mm and a third Ioffe coil with 199 turns, which is offset from the centre of the anti-Helmholtz pair by 22 mm and orthogonal to the quadrupole axis. The QUIC trap has a radial gradient of 172 G/cm and axial curvature is  $162.2\text{ G/cm}^2$ . The offset field of 1.5 G results in trapping harmonic frequencies of  $2 \times 23.9\text{ Hz}$  in the axial and  $2 \times 236.6\text{ Hz}$  in the radial direction for  $^{40}\text{K}$ , while those for  $^{87}\text{Rb}$  are a factor  $(M_{\text{K}}/M_{\text{Rb}})^{1/2} \approx 0.68$ . The typical numbers of atoms for  $^{87}\text{Rb}$  and  $^{40}\text{K}$  we can load inside the QUIC trap are about  $10^8$  and about  $5 \times 10^6$ , respectively. The temperature of both the species is still quite high, ranging from 200 to 300  $\mu\text{K}$ .

Once the atoms are loaded into the magnetic trap, we have an excellent starting point to achieve runaway evaporation. However, sympathetic cooling requires the interspecies scattering cross section large enough for thermalization. For  $^{87}\text{Rb}/^{87}\text{Rb}$  collisions the scattering length is  $98.98(4)a_0$ ,<sup>[11]</sup> whereas for  $^{40}\text{K}/^{87}\text{Rb}$  it is  $-215(10)a_0$ .<sup>[12]</sup> Such promising attractive interaction of  $^{40}\text{K}$ - $^{87}\text{Rb}$  mixtures would allow efficient cooling well below the Fermi temperature. As the first case, we only evaporate  $^{87}\text{Rb}$  atoms to the Bose-Einstein condensation, without  $^{40}\text{K}$  atoms in magnetic trap. Then we load  $^{40}\text{K}$  and  $^{87}\text{Rb}$  atoms into the magnetic trap, cool sympathetically the  $^{40}\text{K}$  atoms to the Fermi degeneracy by means of an efficient thermalization with the evaporatively cooled  $^{87}\text{Rb}$ .

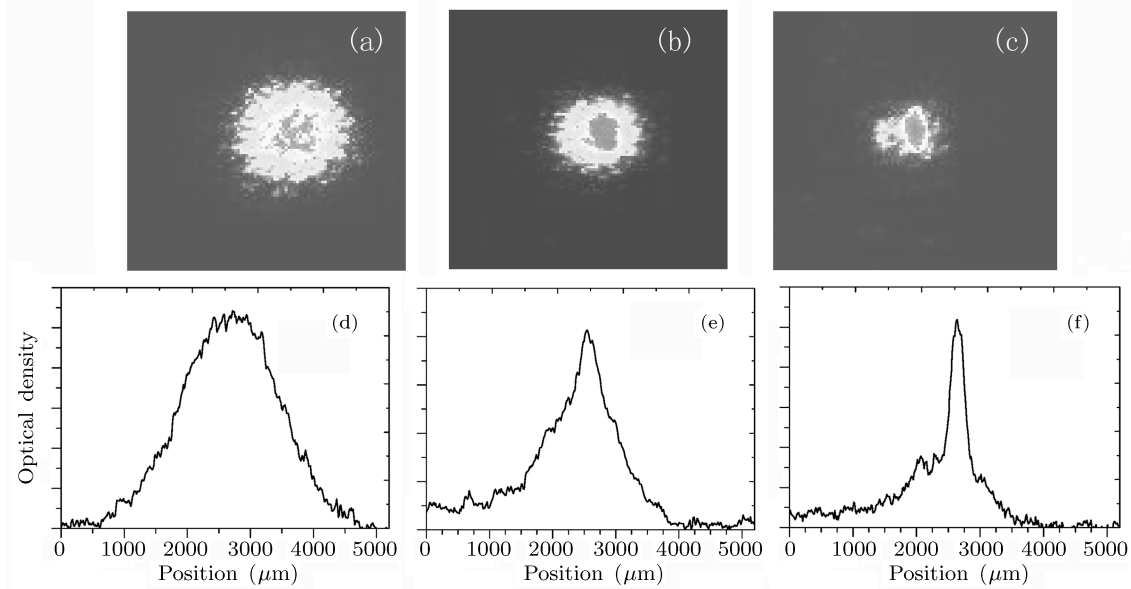


**Fig. 3.** Two-dimensional absorption images showing evidence for BEC after 25 ms time of flight. (a) The velocity distribution of an atomic cloud above the transition point. (b) The difference between the isotropic thermal distribution and elliptical core attributed to the expansion of a dense condensate after the condensate appear. (c) An almost pure condensate left after further evaporative cooling. Here (d), (e), and (f) are the vertically integrated column optical densities of the images corresponding to (a), (b), and (c), respectively.

Over a period of 43 s the rf (radio frequency) is swept from 30 MHz to a final value of 1.0 MHz, we achieved the Bose–Einstein condensation of  $^{87}\text{Rb}$ . Figure 3 shows the formation of the  $^{87}\text{Rb}$  Bose–Einstein condensation. These absorption images are taken with 25 ms expansion time and  $50\ \mu\text{s}$  exposure time. In Fig. 3(a), the atoms are still a thermal cloud. Figure 3(b) shows the appearance of the condensate, in which the isotropic thermal distribution and elliptical core attributed to the expansion of a dense condensate can be clearly seen at the same time. Figure 3(c) shows that the narrow condensate peak becomes more pronounced with no obvious thermal pedestal.

The vertically integrated column optical density of Figs. 3(a), 3(b) and 3(c) are respectively shown in Figs. 3(d), 3(e) and 3(f). Typically, we could cool up to  $1.8 \times 10^5$   $^{87}\text{Rb}$  into a pure condensate. The phase transition occurs at a temperature of  $T_c \approx 500$  nK. In addition, we note that a small condensate peak appears on the left of the main condensate in Figs. 3(c) and 3(f). The reason for this is the slight difference of the switch-off time constant between the Ioffe coil and the quadruple coils during the condensate released from the QUIC trap. The condensate originally in the  $|2, 2\rangle$  state will flip to the other spin state (mainly  $|2, 1\rangle$  state in our experiment) by the Majorana transition.<sup>[13]</sup> Then the different spin states are translated into spatial separation by the magnetic gradient (Stern–Gerlach effect).

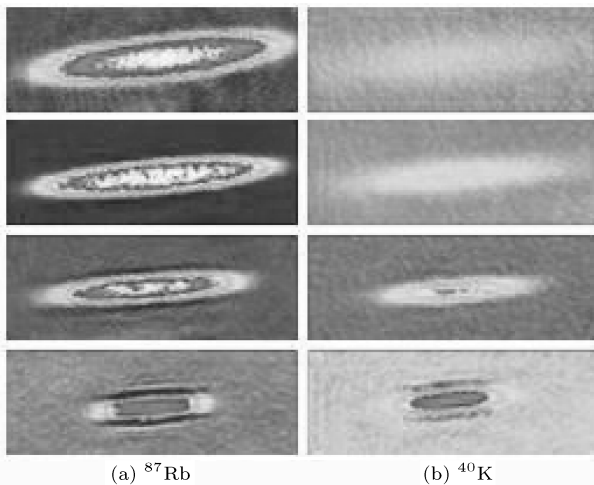


**Fig. 4.** Absorption images of  $^{87}\text{Rb}$  (a) and  $^{40}\text{K}$  (b) atom clouds at different end frequencies of the rubidium evaporation ramp. The density increase and temperature decrease over several orders of magnitude are clearly visible.

Sympathetic cooling of  $^{40}\text{K}$  atoms to quantum degeneracy is performed by selectively evaporating  $^{87}\text{Rb}$  while  $^{40}\text{K}$  is cooled in the bath of  $^{87}\text{Rb}$  atoms. The selectivity of the evaporation process relies on the fact that the gyromagnetic factors of the resonance frequency in the magnetic trap for  $^{87}\text{Rb}$  is about twice the resonance frequency for  $^{40}\text{K}$ . Both  $^{40}\text{K}$  in the  $|F = 9/2, m_F = 9/2\rangle$  state and  $^{87}\text{Rb}$  in the  $|F = 2, m_F = 2\rangle$  state have the same magnetic moment but different numbers of magnetic sublevels respectively in the hyperfine manifold. Thus, they experience the same trapping potential but with an rf-cutoff differing by a factor of 2.25. It is thus possible to restrict the evaporation losses to the rubidium atoms and sympathetically cool the potassium ensemble, which quickly thermalizes with the cold  $^{87}\text{Rb}$  cloud due to the large interspecies collisional elastic

cross section.<sup>[14]</sup>

Absorption images of the trapped  $^{87}\text{Rb}$  (Fig. 4(a)) and  $^{40}\text{K}$  (Fig. 4(b)) gas are taken with 1 ms expansion time and 50 s exposure time. The evaporation is terminated at different trap depths, and the sample is allowed to fully thermalize. The density increase and temperature decrease over several orders of magnitude are clearly visible, which show the efficiency of evaporation cooling.

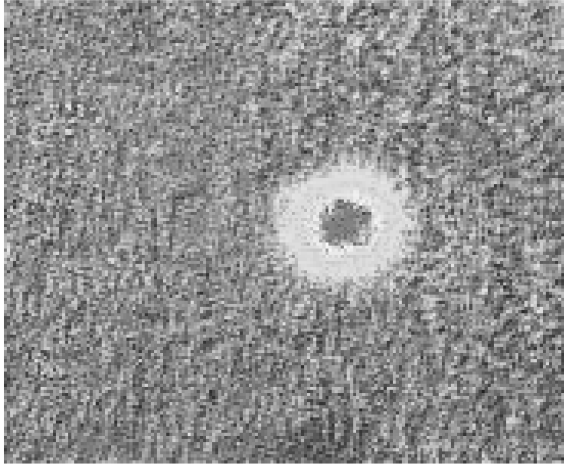


**Fig. 5.**  $^{40}\text{K}$  Fermi degeneracy with 12 ms expansion time, which corresponds to  $T/T_F = 0.5$ .

Using the similar evaporation ramp lasting 43 s with  $\nu_{\text{final}} = 1.0 \text{ MHz}$ , we obtain up to  $7.59 \times 10^5$   $^{40}\text{K}$  Fermi degeneracy, which is shown in Fig. 5. The images are taken with expansion time 12 ms. Then we obtain the fugacity, temperature and atom number by fitting two dimensional Fermi–Dirac profiles to the experimental data.<sup>[14]</sup> From the atom number in the system we can obtain  $T_F = 961 \text{ nK}$  by the function  $T_F = (\hbar\omega/k_B)(6N)^{1/3}$ , where  $\omega$  is the geometric mean of the three oscillation frequencies in the trap,  $N$  is the number of fermions, and  $k_B$  is Boltzmann’s constant. Combined with the atoms temperature, we obtain the degeneracy parameter  $T_v/T_F = 0.50$  and  $T_h/T_F = 0.48$ ,  $T_v$  and  $T_h$  is the vertical and horizontal temperatures. The third value of degeneracy parameter based on fugacity is  $T/T_F = 0.28$ . Thus the horizontal and vertical temperatures agree very well, but both of them do not fully agree with the temperature from the fugacity; the latter is lower, which could be caused by the parameters calibration uncertainty in our experimental system. On the one hand, the number of atoms in the other spin states is small under the imperfect switching-off of the trap. On the other hand, the space separation of different spin states for  $^{40}\text{K}$  is minor compared with the cloud size. Thus we neglect the effect of the imperfect switching-off of a trap in the estimate of the atom number and temperature of  $^{40}\text{K}$  DFG.

Figure 6 shows the one-dimensional profiles of  $^{40}\text{K}$

clouds (Fig. 5). The dotted line is the optical column density as observed in the imaging, integrated along the horizontal direction. The dashed line is a fit to the recorded column densities using an exact semi-classical Fermi–Dirac distribution.<sup>[15]</sup> While the solid line is a hypothetical Maxwell–Boltzmann gas distribution with the same temperature and particle number as the Fermi gas. It shows that the Fermi–Dirac distribution describes the data very well, and the classical fit is narrower and higher than the experimental data. The absolute deviation in the classical fit is a clear signature of the Fermi degeneracy.

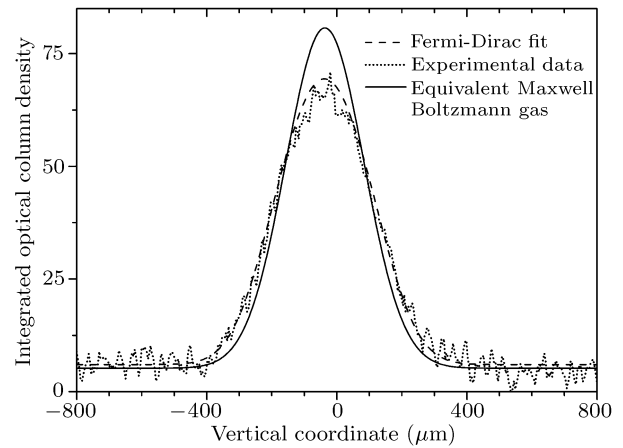


**Fig. 6.** Thermometry for the degenerate Fermi gas.

In summary, we have demonstrated sympathetic cooling of fermionic  $^{40}\text{K}$  via evaporation performed on the bosonic  $^{87}\text{Rb}$  and obtained temperatures of  $0.5T_F$ . This provides us with the starting point for studies of the degenerate  $^{40}\text{K}$  Fermi gas. Further, favourable collisional properties make the  $^{40}\text{K}$ – $^{87}\text{Rb}$  system very promising for studies on the degenerate Bose–Fermi mixtures.

The authors thank Professor Kunchi PENG and Professor Changde Xie for valuable advice and support. Jing Zhang thanks Junming Wang, Baolong Lu and Xiaoji Zhou for useful discussions, Professor Weiping Zhang and Professor Wuming Liu for good advice.

## References

- [1] Chen Q et al 2005 *Phys. Rep.* **412** 1
- [2] Xiong H W et al 2005 *Prog. Phys.* **25** 296 (in Chinese)
- [3] Grimm R et al 2000 *Adv. At. Mol. Opt. Phys.* **42** 95
- [4] Bloch I 2005 *J. Phys. B* **38** S629
- [5] Takamoto M et al 2005 *Nature* **435** 321
- [6] Esslinger T et al 1998 *Phys. Rev. A* **58** R2664
- [7] Wei D et al 2006 *Chin. Phys. Lett.* **24** 679
- [8] Wei D et al 2006 *Acta Phys. Sin.* **55** 6342 (in Chinese)
- [9] Wei D et al 2007 *Chin. Phys. Lett.* **24** 1541
- [10] Goldwin J et al 2002 *Phys. Rev. A* **65** 021402
- [11] van Kempen E G M et al 2002 *Phys. Rev. Lett.* **88** 093201
- [12] Ferlino F et al 2006 *Phys. Rev. A* **73** 040702
- [13] Ma X Q et al 2005 *Chin. Phys. Lett.* **22** 1106
- [14] Ospelkaus C 2006 *PhD Thesis* (University of Hamburg)
- [15] Buttsand D A et al 1997 *Phys. Rev. A* **55** 4346